

**STABILITY ANALYSIS OF
MAGNETOHYDRODYNAMIC FLOW AND HEAT
TRANSFER OVER A MOVING FLAT PLATE IN
FERROFLUIDS WITH SLIP EFFECTS**

NORSHAFIRA BINTI RAMLI

UNIVERSITI SAINS MALAYSIA

2018

**STABILITY ANALYSIS OF
MAGNETOHYDRODYNAMIC FLOW AND HEAT
TRANSFER OVER A MOVING FLAT PLATE IN
FERROFLUIDS WITH SLIP EFFECTS**

by

NORSHAFIRA BINTI RAMLI

**Thesis submitted in fulfilment of the requirements
for the degree of
Doctor of Philosophy**

August 2018

ACKNOWLEDGEMENT



Allah's protection we seek against Satan, the accursed. In the name of Allah, the Most Gracious and the Most Merciful. Alhamdulillah, all praises and gratitudes belong to Allah, the Lord Almighty, the Cherisher and the Sustainer of the world. Blessings and peace be upon the last Prophet, Muhammad s.a.w., his family, and his companions. First of all, I am grateful to Allah for the gift of life, health, determination, strength and ability to complete this thesis.

I wish to express my sincerest, intense thankfulness and indebtedness to my supervisor Dr. Syakila Ahmad, School of Mathematical Sciences, Universiti Sains Malaysia, for her constant inspiration, invaluable suggestion, inexorable assistance and supervision, besides her continuous support throughout my study. Without her help, this thesis work would be surely impossible.

Additionally, I would like to acknowledge Prof. Ioan Pop from Department of Mathematics, Babeş-Bolyai University, Romania for his insightful comments and helpful suggestions throughout the tenure of the work. My sincere gratitude and appreciation to the examiners, Prof. Dr. Roslinda Mohd Nazar, Prof. Norhashidah Hj. Mohd Ali and Dr. Yazariah Mohd Yatim for their constructive comments and suggestions to improve the quality of my thesis.

I am thankful to all my colleagues for their immense help and ideas in completing my thesis work. Your inputs are greatly treasured and I wish the best in your future endeavours. Furthermore, I would also like to express my thanks to all university

members and staffs of School of Mathematical Sciences, Universiti Sains Malaysia, for providing laboratory and library facilities.

The financial supports provided by Universiti Sains Malaysia under the program of Academic Staff Training Scheme (ASTS) and Ministry of Higher Education throughout the course of my study are gratefully acknowledged.

Last but not least, I am so blessed and highly thankful to my husband (Dr. Mu'az Salleh), parents (Hj. Ramli Mohamed and Hjh. W. Zainah W. Hussin), sons (Abdullah Fateh Mu'az and Abdullah Mu'awwidz Mu'az) and my family members for their continuous prayers, love, care, support, encouragement and best cooperation, which inspired me to achieve my goal.

May Allah bless and keep you safe each hour of every day, and be the light that guides you each step of the way.

TABLE OF CONTENTS

Acknowledgement.....	ii
Table of Contents	iv
List of Tables	ix
List of Figures	xiii
List of Abbreviations	xxi
List of Symbols.....	xxii
Abstrak.....	xxix
Abstract	xxxii
CHAPTER 1 – INTRODUCTION.....	1
1.1 Introductory Remarks	1
1.2 Magnetohydrodynamic (MHD).....	3
1.3 Heat Transfer	4
1.3.1 Conduction	4
1.3.2 Convection.....	6
1.3.2(a) Free Convection	6
1.3.2(b) Forced Convection	6
1.3.2(c) Mixed Convection.....	7
1.3.3 Radiation	7
1.4 Nanofluids	8
1.5 Ferrofluids	10
1.6 Boundary Layer Theory	11

1.7	Suction	14
1.8	Slip Condition	16
1.9	Dimensionless Parameters	17
1.9.1	Prandtl Number	18
1.9.2	Reynolds Number	19
1.9.3	Grashof Number	19
1.9.4	Nusselt Number	20
1.9.5	Eckert Number	21
1.9.6	Knudsen Number.....	21
1.10	Motivations of Study	22
1.11	Problem Statement	23
1.12	Objectives and Scope.....	25
1.13	Research Methodology.....	26
1.14	Thesis Outline	27
CHAPTER 2 – LITERATURE REVIEW		29
2.1	Introduction	29
2.2	MHD Flow and Heat Transfer in Ferrofluids.....	29
2.3	Moving Flat Plate.....	35
2.4	Second-order Slip Boundary Condition	41
2.5	Effect of Thermal Radiation	45
2.6	Stability Analysis.....	50
CHAPTER 3 – GOVERNING EQUATIONS, NUMERICAL METHODS AND STABILITY ANALYSIS		56
3.1	Introduction	56

3.2	The Governing Equations of Ferrofluids in the Forced Convection.....	57
3.2.1	Non-dimensional Equations	61
3.2.2	Order of Magnitude Analysis.....	62
3.2.2(a)	Continuity Equation.....	64
3.2.2(b)	Momentum Equation.....	65
3.2.2(c)	Energy Equation.....	70
3.3	Similarity Transformation.....	73
3.4	Numerical Methods.....	77
3.4.1	Shooting Method and Maple Implementation	78
3.4.1(a)	Newton-Raphson Method.....	80
3.4.1(b)	Fourth-order Runge-Kutta Method.....	81
3.4.1(c)	Maple Implementation	84
3.4.2	Collocation Method and Matlab bvp4c Solver	86
3.4.2(a)	Collocation Method	86
3.4.2(b)	Matlab bvp4c Solver.....	88
3.5	Stability Analysis	92
 CHAPTER 4 – MHD FORCED CONVECTION FLOW OVER A MOVING FLAT PLATE IN FERROFLUIDS WITH SUCTION AND SECOND-ORDER SLIP EFFECTS		 99
4.1	Introduction	99
4.2	Basic Equations.....	100
4.3	Stability Analysis	101
4.4	Results and Discussion	102
4.4.1	Considering First-order Slip Effects without Suction	104
4.4.2	Considering Second-order Slip Effects with Suction.....	118

4.5	Conclusions	148
CHAPTER 5 – MHD MIXED CONVECTION FLOW OVER A MOVING FLAT PLATE IN FERROFLUIDS WITH SUCTION AND SLIP EFFECTS		150
5.1	Introduction	150
5.2	The Governing Equations of Ferrofluids in the Mixed Convection	151
5.2.1	Boussinesq Approximation	152
5.2.2	Non-dimensional Equations	154
5.2.3	Order of Magnitude Analysis.....	154
5.3	Basic Equations.....	156
5.4	Stability Analysis	159
5.5	Results and Discussion	161
5.5.1	Assisting Flow Case, $\omega > 0$	176
5.5.2	Opposing Flow Case, $\omega < 0$	185
5.6	Conclusions	193
CHAPTER 6 – MHD MIXED CONVECTION FLOW OVER A MOVING FLAT PLATE IN FERROFLUIDS WITH THERMAL RADIATION, SUCTION AND SECOND-ORDER SLIP EFFECTS		195
6.1	Introduction	195
6.2	The Governing Equations of Ferrofluids in the Mixed Convection with Thermal Radiation.....	196
6.2.1	Non-dimensional Equations	197
6.2.2	Order of Magnitude Analysis.....	197
6.3	Basic Equations.....	199
6.4	Stability Analysis	203

6.5	Results and Discussion	205
6.5.1	Assisting Flow Case, $\omega > 0$	224
6.5.2	Opposing Flow Case, $\omega < 0$	232
6.6	Conclusions	240
CHAPTER 7 – CONCLUSION		242
7.1	Summary of Research	242
7.2	Suggestions for Future Research.....	246
REFERENCES		248
APPENDICES		
LIST OF PUBLICATIONS		

LIST OF TABLES

		Page
Table 1.1	Prandtl number of various fluids	18
Table 4.1	Thermophysical properties of base fluids and magnetic nanoparticles (Khan et al., 2015)	103
Table 4.2	Comparison of $f''(0)$ for $a = 0, 0.5$ and $M = 0, 1$ when $\varphi = 0$, $S = 0$, $\lambda = 0$ and $b = 0$	104
Table 4.3	Value of critical point λ_c for different figures and parameters in water- and kerosene-based ferrofluids	113
Table 4.4	Variation of $Re_x^{1/2} C_f$ with M for different ferroparticles with water- and kerosene-based ferrofluids when $\lambda = -0.83$, $a = 2$ and $\varphi = 0.1$	113
Table 4.5	Variation of $Re_x^{-1/2} Nu_x$ with M for different ferroparticles with water- and kerosene-based ferrofluids when $\lambda = -0.83$, $a = 2$ and $\varphi = 0.1$	113
Table 4.6	Variation of $Re_x^{1/2} C_f$ with φ for different ferroparticles with water- and kerosene-based ferrofluids when $\lambda = -0.92$, $M = 0.02$ and $a = 2$	114
Table 4.7	Variation of $Re_x^{-1/2} Nu_x$ with φ for different ferroparticles with water- and kerosene-based ferrofluids when $\lambda = -0.92$, $M = 0.02$ and $a = 2$	114
Table 4.8	Value of critical point λ_c for different figure and parameter in water- and kerosene-based ferrofluids	133
Table 4.9	Variation of $Re_x^{1/2} C_f$ with M for different ferroparticles with water- and kerosene-based ferrofluids when $\lambda = -6$, $\varphi = 0.1$, $S = 2$, $a = 1$ and $b = -1$	133
Table 4.10	Variation of $Re_x^{-1/2} Nu_x$ with M for different ferroparticles with water- and kerosene-based ferrofluids when $\lambda = -6$, $\varphi = 0.1$, $S = 2$, $a = 1$ and $b = -1$	134

Table 4.11	Variation of $\text{Re}_x^{1/2}C_f$ with S for different ferrofluids with water- and kerosene-based ferrofluids when $\lambda = -6$, $\varphi = 0.1$, $M = 0.02$, $a = 1$ and $b = -1$	134
Table 4.12	Variation of $\text{Re}_x^{-1/2}\text{Nu}_x$ with S for different ferrofluids with water- and kerosene-based ferrofluids when $\lambda = -6$, $\varphi = 0.1$, $M = 0.02$, $a = 1$ and $b = -1$	134
Table 4.13	Variation of $\text{Re}_x^{1/2}C_f$ with a for different ferrofluids with water- and kerosene-based ferrofluids when $\lambda = -3$, $\varphi = 0.1$, $M = 0.02$, $S = 2$ and $b = 0$	135
Table 4.14	Variation of $\text{Re}_x^{-1/2}\text{Nu}_x$ with a for different ferrofluids with water- and kerosene-based ferrofluids when $\lambda = -3$, $\varphi = 0.1$, $M = 0.02$, $S = 2$ and $b = 0$	135
Table 4.15	Variation of $\text{Re}_x^{1/2}C_f$ with b for different ferrofluids with water- and kerosene-based ferrofluids when $\lambda = -3$, $\varphi = 0.1$, $M = 0.02$, $S = 2$ and $a = 0$	136
Table 4.16	Variation of $\text{Re}_x^{-1/2}\text{Nu}_x$ with b for different ferrofluids with water- and kerosene-based ferrofluids when $\lambda = -3$, $\varphi = 0.1$, $M = 0.02$, $S = 2$ and $a = 0$	136
Table 4.17	Variation of $\text{Re}_x^{1/2}C_f$ with φ for different ferrofluids with water- and kerosene-based ferrofluids when $\lambda = -5.5$, $M = 0.02$, $S = 2$, $a = 1$ and $b = -1$	137
Table 4.18	Variation of $\text{Re}_x^{-1/2}\text{Nu}_x$ with φ for different ferrofluids with water- and kerosene-based ferrofluids when $\lambda = -5.5$, $M = 0.02$, $S = 2$, $a = 1$ and $b = -1$	137
Table 4.19	Singularity point of $\text{Re}_x^{-1/2}\text{Nu}_x$ for different figures and parameters with water- and kerosene-based ferrofluids	138
Table 4.20	Smallest eigenvalues ζ for Fe_3O_4 , CoFe_2O_4 and $\text{Mn-ZnFe}_2\text{O}_4$ ferrofluids at several values of λ (< 0 , a plate moving towards the origin), with various values of M , when $S = 2$, $a = 1$, $b = -1$, $\varphi = 0.1$ and $\text{Pr} = 6.2$ (water-based ferrofluid)	147
Table 5.1	Value of critical point ω_{c1} and ω_{c2} for different figure and parameter in water- and kerosene-based ferrofluids	174
Table 5.2	Singularity point of $\text{Re}_x^{-1/2}\text{Nu}_x$ for different figures and parameters with water- and kerosene-based ferrofluids	174

Table 5.3	Smallest eigenvalues ζ for Fe_3O_4 , CoFe_2O_4 and $\text{Mn-ZnFe}_2\text{O}_4$ ferroparticles at several values of ω (< 0 , opposing flow), with various values of M , when $S = 3$, $\lambda = -7$, $D = 1$, $\varphi = 0.1$ and $\text{Pr} = 6.2$ (water-based ferrofluid)	175
Table 5.4	Variation of $\text{Re}_x^{1/2}C_f$ with ω (> 0 , assisting flow) for different ferroparticles with water- and kerosene-based ferrofluids when $\varphi = 0.1$, $M = 0.02$, $\lambda = -7$, $S = 3$ and $D = 1$	181
Table 5.5	Variation of $\text{Re}_x^{-1/2}\text{Nu}_x$ with ω (> 0 , assisting flow) for different ferroparticles with water- and kerosene-based ferrofluids when $\varphi = 0.1$, $M = 0.02$, $\lambda = -7$, $S = 3$ and $D = 1$	182
Table 5.6	Variation of $\text{Re}_x^{1/2}C_f$ with ω (< 0 , opposing flow) for different ferroparticles with water- and kerosene-based ferrofluids when $\varphi = 0.1$, $M = 0.02$, $\lambda = -7$, $S = 3$ and $D = 1$	189
Table 5.7	Variation of $\text{Re}_x^{-1/2}\text{Nu}_x$ with ω (< 0 , opposing flow) for different ferroparticles with water- and kerosene-based ferrofluids when $\varphi = 0.1$, $M = 0.02$, $\lambda = -7$, $S = 3$ and $a = 1$	190
Table 6.1	Value of critical point ω_{c1} and ω_{c2} for different figure and parameter in water- and kerosene-based ferrofluids	221
Table 6.2	Singularity point of $\text{Re}_x^{-1/2}\text{Nu}_x$ for different figures and parameters with water- and kerosene-based ferrofluids	222
Table 6.3	Smallest eigenvalues ζ for Fe_3O_4 , CoFe_2O_4 and $\text{Mn-ZnFe}_2\text{O}_4$ ferroparticles at several values of ω (< 0 , opposing flow), with various values of M , when $S = 3$, $\lambda = -14$, $\varphi = 0.1$, $D = 1$, $E = -1$, $R = 10$ and $\text{Pr} = 6.2$ (water-based ferrofluid)	223
Table 6.4	Variation of $\text{Re}_x^{1/2}C_f$ with ω (> 0 , assisting flow) for different ferroparticles with water- and kerosene-based ferrofluids when $\varphi = 0.1$, $M = 0.02$, $R = 10$, $\lambda = -14$, $S = 3$, $D = 1$ and $E = -1$	228
Table 6.5	Variation of $\text{Re}_x^{-1/2}\text{Nu}_x$ with ω (> 0 , assisting flow) for different ferroparticles with water- and kerosene-based ferrofluids when $\varphi = 0.1$, $M = 0.02$, $R = 10$, $\lambda = -14$, $S = 3$, $D = 1$ and $E = -1$	229

Table 6.6	Variation of $\text{Re}_x^{1/2} C_f$ with ω (< 0 , opposing flow) for different ferroparticles with water- and kerosene-based ferrofluids when $\varphi = 0.1$, $M = 0.02$, $R = 10$, $\lambda = -14$, $S = 3$, $D = 1$ and $E = -1$	236
Table 6.7	Variation of $\text{Re}_x^{-1/2} \text{Nu}_x$ with ω (< 0 , opposing flow) for different ferroparticles with water- and kerosene-based ferrofluids when $\varphi = 0.1$, $M = 0.02$, $R = 10$, $\lambda = -14$, $S = 3$, $D = 1$ and $E = -1$	237

LIST OF FIGURES

		Page
Figure 1.1	Schematic cross-section of nanofluids structure (Sridhara et al., 2009)	8
Figure 1.2	Components of ferrofluids (Rene, 2014)	11
Figure 1.3	Regions of the fluid flow (Anderson, 2005)	12
Figure 1.4	Velocity and thermal boundary layers (Malvandi et al., 2013)	14
Figure 1.5	Permeability, (a) rock and (b) sand (Edwards, 2016)	15
Figure 1.6	Slip length, L_s , for simple shear flow along a flat plate (Thompson and Troian, 1997; McCormack, 2012)	17
Figure 1.7	Flow chart of methodology	27
Figure 4.1	Physical model and coordinate system	101
Figure 4.2	Variation of $Re_x^{1/2}C_f$ with λ for Fe_3O_4 , (a) water-based ferrofluid, $Pr = 6.2$ and (b) kerosene-based ferrofluid, $Pr = 21$, when $a = 2$, $\varphi = 0.1$ and with varying M	107
Figure 4.3	Variation of $Re_x^{-1/2}Nu_x$ with λ for Fe_3O_4 , (a) water-based ferrofluid, $Pr = 6.2$ and (b) kerosene-based ferrofluid, $Pr = 21$, when $a = 2$, $\varphi = 0.1$ and with varying M	108
Figure 4.4	Variation of $Re_x^{1/2}C_f$ with λ for Fe_3O_4 , (a) water-based ferrofluid, $Pr = 6.2$ and (b) kerosene-based ferrofluid, $Pr = 21$, when $M = 0.02$, $\varphi = 0.1$ and with varying a	109
Figure 4.5	Variation of $Re_x^{-1/2}Nu_x$ with λ for Fe_3O_4 , (a) water-based ferrofluid, $Pr = 6.2$ and (b) kerosene-based ferrofluid, $Pr = 21$, when $M = 0.02$, $\varphi = 0.1$ and with varying a	110
Figure 4.6	Variation of $Re_x^{1/2}C_f$ with λ for Fe_3O_4 , (a) water-based ferrofluid, $Pr = 6.2$ and (b) kerosene-based ferrofluid, $Pr = 21$, when $M = 0.02$, $a = 2$ and with varying φ	111
Figure 4.7	Variation of $Re_x^{-1/2}Nu_x$ with λ for Fe_3O_4 , (a) water-based ferrofluid, $Pr = 6.2$ and (b) kerosene-based ferrofluid, $Pr = 21$, when $M = 0.02$, $a = 2$ and with varying φ	112

Figure 4.8	Dimensionless (a) velocity profiles $f'(\eta)$ and (b) temperature profiles $\theta(\eta)$, for several values of M , Fe_3O_4 , when $\varphi = 0.1$, $\lambda = -0.83$ and $a = 2$	115
Figure 4.9	Dimensionless (a) velocity profiles $f'(\eta)$ and (b) temperature profiles $\theta(\eta)$, for several values of a , Fe_3O_4 , when $\varphi = 0.1$, $M = 0.02$, $\lambda = -0.92$	116
Figure 4.10	Dimensionless (a) velocity profiles $f'(\eta)$ and (b) temperature profiles $\theta(\eta)$, for several values of φ , Fe_3O_4 , when $M = 0.02$, $\lambda = -0.92$ and $a = 2$	117
Figure 4.11	Variation of $\text{Re}_x^{1/2}C_f$ with λ for Fe_3O_4 , (a) water-based ferrofluid, $\text{Pr} = 6.2$ and (b) kerosene-based ferrofluid, $\text{Pr} = 21$, when $S = 2$, $a = 1$, $b = -1$, $\varphi = 0.1$ and with varying M	121
Figure 4.12	Variation of $\text{Re}_x^{-1/2}\text{Nu}_x$ with λ for Fe_3O_4 , (a) water-based ferrofluid, $\text{Pr} = 6.2$ and (b) kerosene-based ferrofluid, $\text{Pr} = 21$, when $S = 2$, $a = 1$, $b = -1$, $\varphi = 0.1$ and with varying M	122
Figure 4.13	Variation of $\text{Re}_x^{1/2}C_f$ with S for Fe_3O_4 , (a) water-based ferrofluid, $\text{Pr} = 6.2$ and (b) kerosene-based ferrofluid, $\text{Pr} = 21$, when $\lambda = -3$, $a = 1$, $b = -1$, $\varphi = 0.1$ and with varying M	123
Figure 4.14	Variation of $\text{Re}_x^{-1/2}\text{Nu}_x$ with S for Fe_3O_4 , (a) water-based ferrofluid, $\text{Pr} = 6.2$ and (b) kerosene-based ferrofluid, $\text{Pr} = 21$, when $\lambda = -3$, $a = 1$, $b = -1$, $\varphi = 0.1$ and with varying M	124
Figure 4.15	Variation of $\text{Re}_x^{1/2}C_f$ with λ for Fe_3O_4 , (a) water-based ferrofluid, $\text{Pr} = 6.2$ and (b) kerosene-based ferrofluid, $\text{Pr} = 21$, when $M = 0.02$, $a = 1$, $b = -1$, $\varphi = 0.1$ and with varying S	125
Figure 4.16	Variation of $\text{Re}_x^{-1/2}\text{Nu}_x$ with λ for Fe_3O_4 , (a) water-based ferrofluid, $\text{Pr} = 6.2$ and (b) kerosene-based ferrofluid, $\text{Pr} = 21$, when $M = 0.02$, $a = 1$, $b = -1$, $\varphi = 0.1$ and with varying S	126
Figure 4.17	Variation of $\text{Re}_x^{1/2}C_f$ with λ for Fe_3O_4 , (a) water-based ferrofluid, $\text{Pr} = 6.2$ and (b) kerosene-based ferrofluid, $\text{Pr} = 21$, when $M = 0.02$, $S = 2$, $b = 0$, $\varphi = 0.1$ and with varying a	127
Figure 4.18	Variation of $\text{Re}_x^{-1/2}\text{Nu}_x$ with λ for Fe_3O_4 , (a) water-based ferrofluid, $\text{Pr} = 6.2$ and (b) kerosene-based ferrofluid, $\text{Pr} = 21$, when $M = 0.02$, $S = 2$, $b = 0$, $\varphi = 0.1$ and with varying a	128

Figure 4.19	Variation of $\text{Re}_x^{1/2}C_f$ with λ for Fe_3O_4 , (a) water-based ferrofluid, $\text{Pr} = 6.2$ and (b) kerosene-based ferrofluid, $\text{Pr} = 21$, when $M = 0.02$, $S = 2$, $a = 0$, $\varphi = 0.1$ and with varying b	129
Figure 4.20	Variation of $\text{Re}_x^{-1/2}\text{Nu}_x$ with λ for Fe_3O_4 , (a) water-based ferrofluid, $\text{Pr} = 6.2$ and (b) kerosene-based ferrofluid, $\text{Pr} = 21$, when $M = 0.02$, $S = 2$, $a = 0$, $\varphi = 0.1$ and with varying b	130
Figure 4.21	Variation of $\text{Re}_x^{1/2}C_f$ with λ for Fe_3O_4 , (a) water-based ferrofluid, $\text{Pr} = 6.2$ and (b) kerosene-based ferrofluid, $\text{Pr} = 21$, when $M = 0.02$, $S = 2$, $a = 1$, $b = -1$ and with varying φ	131
Figure 4.22	Variation of $\text{Re}_x^{-1/2}\text{Nu}_x$ with λ for Fe_3O_4 , (a) water-based ferrofluid, $\text{Pr} = 6.2$ and (b) kerosene-based ferrofluid, $\text{Pr} = 21$, when $M = 0.02$, $S = 2$, $a = 1$, $b = -1$ and with varying φ	132
Figure 4.23	Dimensionless (a) velocity profiles $f'(\eta)$ and (b) temperature profiles $\theta(\eta)$, for several values of λ , Fe_3O_4 , when $\varphi = 0.1$, $a = 1$, $b = -1$, $M = 0.02$, $S = 2$ and different based ferrofluids	139
Figure 4.24	Dimensionless (a) velocity profiles $f'(\eta)$ and (b) temperature profiles $\theta(\eta)$, for several values of λ , Fe_3O_4 , when $\varphi = 0.1$, $a = 1$, $b = -1$, $M = 0.02$, $S = 2$ and different based ferrofluids	140
Figure 4.25	Dimensionless (a) velocity profiles $f'(\eta)$ and (b) temperature profiles $\theta(\eta)$, for several values of M , Fe_3O_4 , when $\varphi = 0.1$, $a = 1$, $b = -1$, $S = 2$, $\lambda = -6.2$ and different based ferrofluids	141
Figure 4.26	Dimensionless (a) velocity profiles $f'(\eta)$ and (b) temperature profiles $\theta(\eta)$, for several values of M , Fe_3O_4 , when $\varphi = 0.1$, $a = 1$, $b = -1$, $S = 2$, $\lambda = -4.8$ and different based ferrofluids	142
Figure 4.27	Dimensionless (a) velocity profiles $f'(\eta)$ and (b) temperature profiles $\theta(\eta)$, for several values of S , Fe_3O_4 , when $\varphi = 0.1$, $a = 1$, $b = -1$, $M = 0.02$, $\lambda = -5.7$ and different based ferrofluids	143
Figure 4.28	Dimensionless (a) velocity profiles $f'(\eta)$ and (b) temperature profiles $\theta(\eta)$, for several values of a , Fe_3O_4 , when $\varphi = 0.1$, $b = 0$, $M = 0.02$, $S = 2$, $\lambda = -3$ and different based ferrofluids	144

Figure 4.29	Dimensionless (a) velocity profiles $f'(\eta)$ and (b) temperature profiles $\theta(\eta)$, for several values of b , Fe_3O_4 , when $\varphi = 0.1$, $a = 0$, $M = 0.02$, $S = 2$, $\lambda = -3$ and different based ferrofluids	145
Figure 4.30	Dimensionless (a) velocity profiles $f'(\eta)$ and (b) temperature profiles $\theta(\eta)$, for several values of φ , Fe_3O_4 , when $a = 1$, $b = -1$, $M = 0.02$, $S = 2$, $\lambda = -5.7$ and different based ferrofluids	146
Figure 4.31	Plot of smallest eigenvalues ζ as a function of λ	148
Figure 5.1	Physical model and coordinate system	157
Figure 5.2	Variation of $\text{Re}_x^{1/2}C_f$ with ω for Fe_3O_4 , (a) water-based ferrofluid, $\text{Pr} = 6.2$ and (b) kerosene-based ferrofluid, $\text{Pr} = 21$, when $S = 3$, $\lambda = -7.2$, $D = 1$, $\varphi = 0.1$ and with varying M	166
Figure 5.3	Variation of $\text{Re}_x^{-1/2}\text{Nu}_x$ with ω for Fe_3O_4 , (a) water-based ferrofluid, $\text{Pr} = 6.2$ and (b) kerosene-based ferrofluid, $\text{Pr} = 21$, when $S = 3$, $\lambda = -7.2$, $D = 1$, $\varphi = 0.1$ and with varying M	167
Figure 5.4	Variation of $\text{Re}_x^{1/2}C_f$ with ω for Fe_3O_4 , (a) water-based ferrofluid, $\text{Pr} = 6.2$ and (b) kerosene-based ferrofluid, $\text{Pr} = 21$, when $M = 0.02$, $\lambda = -7.2$, $D = 1$, $\varphi = 0.1$ and with varying S	168
Figure 5.5	Variation of $\text{Re}_x^{-1/2}\text{Nu}_x$ with ω for Fe_3O_4 , (a) water-based ferrofluid, $\text{Pr} = 6.2$ and (b) kerosene-based ferrofluid, $\text{Pr} = 21$, when $M = 0.02$, $\lambda = -7.2$, $D = 1$, $\varphi = 0.1$ and with varying S	169
Figure 5.6	Variation of $\text{Re}_x^{1/2}C_f$ with ω for Fe_3O_4 , (a) water-based ferrofluid, $\text{Pr} = 6.2$ and (b) kerosene-based ferrofluid, $\text{Pr} = 21$, when $M = 0.02$, $S = 3$, $\lambda = -7.2$, $\varphi = 0.1$ and with varying D	170
Figure 5.7	Variation of $\text{Re}_x^{-1/2}\text{Nu}_x$ with ω for Fe_3O_4 , (a) water-based ferrofluid, $\text{Pr} = 6.2$ and (b) kerosene-based ferrofluid, $\text{Pr} = 21$, when $M = 0.02$, $S = 3$, $\lambda = -7.2$, $\varphi = 0.1$ and with varying D	171
Figure 5.8	Variation of $\text{Re}_x^{1/2}C_f$ with ω for Fe_3O_4 , (a) water-based ferrofluid, $\text{Pr} = 6.2$ and (b) kerosene-based ferrofluid, $\text{Pr} = 21$, when $M = 0.02$, $S = 3$, $\lambda = -6.6$, $D = 1$ and with varying φ	172

Figure 5.9	Variation of $Re_x^{-1/2}Nu_x$ with ω for Fe_3O_4 , (a) water-based ferrofluid, $Pr = 6.2$ and (b) kerosene-based ferrofluid, $Pr = 21$, when $M = 0.02$, $S = 3$, $\lambda = -6.6$, $D = 1$ and with varying φ	173
Figure 5.10	Plot of smallest eigenvalues ζ as a function of ω	176
Figure 5.11	Variation of $Re_x^{1/2}C_f$ with λ for Fe_3O_4 , (a) water-based ferrofluid, $Pr = 6.2$ and (b) kerosene-based ferrofluid, $Pr = 21$, when $\omega = 0.1$ (assisting flow), $S = 3$, $D = 1$, $\varphi = 0.1$ and with varying M	179
Figure 5.12	Variation of $Re_x^{-1/2}Nu_x$ with λ for Fe_3O_4 , (a) water-based ferrofluid, $Pr = 6.2$, (b) kerosene-based ferrofluid, $Pr = 21$ and (c) enlargement of the area in (b), when $\omega = 0.1$ (assisting flow), $S = 3$, $D = 1$, $\varphi = 0.1$ and with varying M	181
Figure 5.13	Dimensionless (a) velocity profiles $f'(\eta)$ and (b) temperature profiles $\theta(\eta)$, for several values of M , Fe_3O_4 , when $\omega = 0.1$ (>0 , assisting flow), $\varphi = 0.1$, $S = 3$, $\lambda = -7.2$ and $D = 1$	183
Figure 5.14	Dimensionless (a) velocity profiles $f'(\eta)$ and (b) temperature profiles $\theta(\eta)$, for several values of ω (>0 , assisting flow), Fe_3O_4 , when $M = 0.02$, $\varphi = 0.1$, $S = 3$, $\lambda = -7$ and $D = 1$	184
Figure 5.15	Variation of $Re_x^{1/2}C_f$ with λ for Fe_3O_4 , (a) water-based ferrofluid, $Pr = 6.2$ and (b) kerosene-based ferrofluid, $Pr = 21$, when $\omega = -0.1$ (opposing flow), $S = 3$, $D = 1$, $\varphi = 0.1$ and with varying M	187
Figure 5.16	Variation of $Re_x^{-1/2}Nu_x$ with λ for Fe_3O_4 , (a) water-based ferrofluid, $Pr = 6.2$, (b) kerosene-based ferrofluid, $Pr = 21$ and (c) enlargement of the area in (b), when $\omega = -0.1$, $S = 3$, $D = 1$, $\varphi = 0.1$ and with varying M	189
Figure 5.17	Dimensionless (a) velocity profiles $f'(\eta)$ and (b) temperature profiles $\theta(\eta)$, for several values of M , Fe_3O_4 , when $\omega = -0.1$ (<0 , opposing flow), $\varphi = 0.1$, $S = 3$, $\lambda = -6.6$ and $D = 1$	191
Figure 5.18	Dimensionless (a) velocity profiles $f'(\eta)$ and (b) temperature profiles $\theta(\eta)$, for several values of ω (<0 , opposing flow), Fe_3O_4 , when $M = 0.02$, $\varphi = 0.1$, $S = 3$, $\lambda = -7$ and $D = 1$	192

Figure 6.1	Physical model and coordinate system	201
Figure 6.2	Variation of $Re_x^{1/2}C_f$ with ω for Fe_3O_4 , (a) water-based ferrofluid, $Pr = 6.2$ and (b) kerosene-based ferrofluid, $Pr = 21$, when $S = 3$, $\lambda = -14.5$, $D = 1$, $E = -1$, $\phi = 0.1$, $R = 10$ and with varying M	209
Figure 6.3	Variation of $Re_x^{-1/2}Nu_x$ with ω for Fe_3O_4 , (a) water-based ferrofluid, $Pr = 6.2$ and (b) kerosene-based ferrofluid, $Pr = 21$, when $S = 3$, $\lambda = -14.5$, $D = 1$, $E = -1$, $\phi = 0.1$, $R = 10$ and with varying M	210
Figure 6.4	Variation of $Re_x^{1/2}C_f$ with ω for Fe_3O_4 , (a) water-based ferrofluid, $Pr = 6.2$ and (b) kerosene-based ferrofluid, $Pr = 21$, when $M = 0.02$, $\omega = 0.1$, $S = 3$, $\lambda = -14.8$, $D = 1$, $E = -1$, $\phi = 0.1$ and with varying R	211
Figure 6.5	Variation of $Re_x^{-1/2}Nu_x$ with ω for Fe_3O_4 , (a) water-based ferrofluid, $Pr = 6.2$ and (b) kerosene-based ferrofluid, $Pr = 21$, when $M = 0.02$, $S = 3$, $\lambda = -14.8$, $D = 1$, $E = -1$, $\phi = 0.1$ and with varying R	212
Figure 6.6	Variation of $Re_x^{1/2}C_f$ with ω for Fe_3O_4 , (a) water-based ferrofluid, $Pr = 6.2$ and (b) kerosene-based ferrofluid, $Pr = 21$, when $M = 0.02$, $\lambda = -14.8$, $D = 1$, $E = -1$, $\phi = 0.1$, $R = 10$ and with varying S	213
Figure 6.7	Variation of $Re_x^{-1/2}Nu_x$ with ω for Fe_3O_4 , (a) water-based ferrofluid, $Pr = 6.2$ and (b) kerosene-based ferrofluid, $Pr = 21$, when $M = 0.02$, $\lambda = -14.8$, $D = 1$, $E = -1$, $\phi = 0.1$, $R = 10$ and with varying S	214
Figure 6.8	Variation of $Re_x^{1/2}C_f$ with ω for Fe_3O_4 , (a) water-based ferrofluid, $Pr = 6.2$ and (b) kerosene-based ferrofluid, $Pr = 21$, when $M = 0.02$, $S = 3$, $\lambda = -7.2$, $E = 0$, $\phi = 0.1$, $R = 10$ and with varying D	215
Figure 6.9	Variation of $Re_x^{-1/2}Nu_x$ with ω for Fe_3O_4 , (a) water-based ferrofluid, $Pr = 6.2$ and (b) kerosene-based ferrofluid, $Pr = 21$, when $M = 0.02$, $S = 3$, $\lambda = -7.2$, $E = 0$, $\phi = 0.1$, $R = 10$ and with varying D	216
Figure 6.10	Variation of $Re_x^{1/2}C_f$ with ω for Fe_3O_4 , (a) water-based ferrofluid, $Pr = 6.2$ and (b) kerosene-based ferrofluid, $Pr = 21$, when $M = 0.02$, $S = 3$, $\lambda = -10$, $D = 0$, $\phi = 0.1$, $R = 10$ and with varying E	217

Figure 6.11	Variation of $Re_x^{-1/2}Nu_x$ with ω for Fe_3O_4 , (a) water-based ferrofluid, $Pr = 6.2$ and (b) kerosene-based ferrofluid, $Pr = 21$, when $M = 0.02$, $S = 3$, $\lambda = -10$, $D = 0$, $\varphi = 0.1$, $R = 10$ and with varying E	218
Figure 6.12	Variation of $Re_x^{1/2}C_f$ with ω for Fe_3O_4 , (a) water-based ferrofluid, $Pr = 6.2$ and (b) kerosene-based ferrofluid, $Pr = 21$, when $M = 0.02$, $S = 3$, $\lambda = -12.7$, $D = 1$, $E = -1$, $R = 10$ and with varying φ	219
Figure 6.13	Variation of $Re_x^{-1/2}Nu_x$ with ω for Fe_3O_4 , (a) water-based ferrofluid, $Pr = 6.2$ and (b) kerosene-based ferrofluid, $Pr = 21$, when $M = 0.02$, $S = 3$, $\lambda = -12.7$, $D = 1$, $E = -1$, $R = 10$ and with varying φ	220
Figure 6.14	Plot of smallest eigenvalues ζ as a function of ω	224
Figure 6.15	Variation of $Re_x^{1/2}C_f$ with S for Fe_3O_4 , (a) water-based ferrofluid, $Pr = 6.2$ and (b) kerosene-based ferrofluid, $Pr = 21$, when $\omega = 0.1$ (assisting flow), $M = 0.02$, $\varphi = 0.1$, $\lambda = -14.5$, $D = 1$, $E = -1$ and with varying R	226
Figure 6.16	Variation of $Re_x^{-1/2}Nu_x$ with S for Fe_3O_4 , (a) water-based ferrofluid, $Pr = 6.2$ and (b) kerosene-based ferrofluid, $Pr = 21$ when $\omega = 0.1$ (assisting flow), $M = 0.02$, $\varphi = 0.1$, $\lambda = -14.5$, $D = 1$, $E = -1$ and with varying R	227
Figure 6.17	Dimensionless (a) velocity profiles $f'(\eta)$ and (b) temperature profiles $\theta(\eta)$, for several values of R , Fe_3O_4 , when $\omega = 0.1$ (>0 , assisting flow), $\varphi = 0.1$, $M = 0.02$, $S = 3$, $\lambda = -14.5$, $D = 1$ and $E = -1$	230
Figure 6.18	Dimensionless (a) velocity profiles $f'(\eta)$ and (b) temperature profiles $\theta(\eta)$, for several values of ω (>0 , assisting flow), Fe_3O_4 , when $M = 0.02$, $\varphi = 0.1$, $R = 10$, $S = 3$, $\lambda = -14$, $D = 1$ and $E = -1$	231
Figure 6.19	Variation of $Re_x^{1/2}C_f$ with S for Fe_3O_4 , (a) water-based ferrofluid, $Pr = 6.2$ and (b) kerosene-based ferrofluid, $Pr = 21$, when $\omega = -0.008$ (opposing flow), $M = 0.02$, $\varphi = 0.1$, $\lambda = -14.5$, $D = 1$, $E = -1$ and with varying R	234
Figure 6.20	Variation of $Re_x^{-1/2}Nu_x$ with λ for Fe_3O_4 , (a) water-based ferrofluid, $Pr = 6.2$, (b) kerosene-based ferrofluid, $Pr = 21$ when $\omega = -0.008$ (opposing flow), $M = 0.02$, $\varphi = 0.1$, $\lambda = -14.5$, $D = 1$, $E = -1$ and with varying R	235

- Figure 6.21 Dimensionless (a) velocity profiles $f'(\eta)$ and (b) temperature profiles $\theta(\eta)$, for several values of R , Fe_3O_4 , when $\omega = -0.008$ (<0 , opposing flow), $\varphi = 0.1$, $M = 0.02$, $S = 3$, $\lambda = -14.5$, $D = 1$ and $E = -1$ 238
- Figure 6.22 Dimensionless (a) velocity profiles $f'(\eta)$ and (b) temperature profiles $\theta(\eta)$, for several values of ω (<0 , opposing flow), Fe_3O_4 , when $M = 0.02$, $\varphi = 0.1$, $R = 10$, $S = 3$, $\lambda = -14$, $D = 1$ and $E = -1$ 239

LIST OF ABBREVIATIONS

BVP Boundary Value Problem

IVP Initial Value Problem

ODEs Ordinary Differential Equations

PDEs Partial Differential Equations

RK4 Runge-Kutta fourth-order numerical method

wb water-based fluid

kb kerosene-based fluid

LIST OF SYMBOLS

a	first-order surface slip parameter (forced convection)
A_1, A_2	given number
b	second-order surface slip parameter (forced convection)
B	scalar of total magnetic field
\mathbf{B}	vector of total magnetic field
B_0	strength of the applied magnetic field
C_f	skin friction coefficient
C_i	distinct real numbers
C_p	specific heat at a constant temperature
$(C_p)_{nf}$	specific heat of nanofluid
D	dimensionless first-order slip parameter (mixed convection)
E	dimensionless second-order slip parameter (mixed convection)
\mathbf{E}	electric field intensity
Ec	Eckert number
$f(\eta)$	dimensionless stream function
$F(\eta)$	small relative to stream function
$\mathbf{F}_{buoyancy}$	buoyancy force
$\mathbf{F}_{magnetic}$	magnetic force
g	gravity acceleration

$G(\eta)$	small relative to temperature function
Gr	Grashof number
h	heat transfer coefficient
h^*	step length
J	electric current of density
k	thermal conductivity
k_f	thermal conductivity of the fluid
k_s	thermal conductivity of the solid
k_{nf}	thermal conductivity of the nanofluid
k_{nf}^*	mean absorption coefficient
Kn	Knudsen number
L	characteristic length of the sheet
M	magnetic parameter
n	quality parameter
N	slip factor velocity
Nu	Nusselt number
O	order
p	pressure
p_d	dynamic pressure
p_h	hydrostatic pressure
p^*	dimensionless pressure

P	derivative of function
Pr	Prandtl number
q	heat flux
q_R	radiation heat flux
q_R^*	dimensionless radiation heat flux
q_w	surface heat flux
P	derivative of function
r	residual
R	radiation parameter
Re	Reynolds number
Re_x	local Reynolds number
s_l	dimensionless slip parameter (forced convection)
S	mass transfer parameter
S_c	critical point of mass transfer parameter
S_{si}	singularities of the mass transfer parameter
t	time
t^*	dimensionless time
T	temperature
T_∞	temperature of the ambient fluid
T_w	temperature of the plate
u, v	velocity components along x - and y -axes

u^*, v^*	dimensionless velocity components along x - and y -axes
u_w	surface velocity
u_{slip}	surface slip velocity
U	fluid velocity respect to the object
U_∞	free stream velocity
v_w	mass flux velocity
\mathbf{V}	velocity field
W	initial guess
x, y	Cartesian coordinates
y_a	boundary conditions at $y = 0$
y_b	boundary conditions at $y \rightarrow \infty$
Y	approximate solution

Greek Letters

α	thermal diffusivity
α_1, α_2	variables
α_f	thermal diffusivity of the fluid
α_{nf}	thermal diffusivity of the nanofluid
β	thermal expansion coefficient
γ	first-order surface velocity slip (forced convection)
Γ	independent variable

δ	boundary layer thickness
δ^*	dimensionless boundary layer thickness
δ_V	velocity boundary layer thickness
δ_T	thermal boundary layer thickness
δ_T^*	dimensionless thermal boundary layer thickness
ζ	eigenvalue parameter
η	independent similarity variable
θ^*	dimensionless temperature
$\theta(\eta)$	dimensionless temperature function
ϑ	molecular mean free path
ι	slip parameter (forced convection)
λ	moving parameter
λ_c	critical point of moving parameter
Λ	momentum accommodation coefficient
μ	dynamic viscosity
μ_f	dynamic viscosity of the fluid
μ_s	dynamic viscosity of the solid
μ_{nf}	dynamic viscosity of the nanofluid
ν	kinematic viscosity
ν_f	kinematic viscosity of the fluid
ν_{nf}	kinematic viscosity of the nanofluid

ξ	independent variable
π	angle
ρ	density
ρ_f	density of the fluid
ρ_s	density of the solid
ρ_{nf}	density of the nanofluid
$(\rho C_p)_f$	heat capacity of the fluid
$(\rho C_p)_s$	heat capacity of the solid
$(\rho C_p)_{nf}$	heat capacity of the nanofluid
ρ_∞	density of the ambient fluid
σ	electrical conductivity
σ^*	Stefan-Boltzmann constant
τ	dimensionless time variable
τ_w	skin friction along the plate
Υ	second-order surface velocity slip (mixed convection)
ϕ	given function
Φ	basic function
φ	volume fraction of solid particle
χ	second-order surface velocity slip (forced convection)
ψ	stream function
ω	mixed convection parameter

ω_{min}	lower bound of mixed convection flow regime
ω_{max}	upper bound of mixed convection flow regime
Ω	first-order surface velocity slip (mixed convection)

Subscripts

c	critical value
f	fluid fraction
min	lower bound
max	upper bound
nf	nanofluid fraction
s	solid fraction
si	singularity point
w	condition at the surface
∞	ambient/free stream condition

Superscripts

'	differentiation with respect to η
*	dimensionless variables

**ANALISIS KESTABILAN BAGI ALIRAN DAN PEMINDAHAN HABA
MAGNETOHIDRODINAMIK PADA PLAT RATA BERGERAK DI DALAM
FERROBENDALIR DENGAN KESAN GELINCIR**

ABSTRAK

Satu kajian mengenai analisis kestabilan pada aliran lapisan sempadan telah menjadi tumpuan dalam bidang dinamik bendalir. Analisis ini adalah penting kerana ia membantu untuk mengenal pasti penyelesaian mana yang stabil jika terdapat penyelesaian yang tidak unik di dalam pengiraan. Dalam tesis ini, analisis kestabilan digunakan pada masalah aliran mantap dua dimensi berlamina magnetohidrodinamik (MHD) dan pemindahan haba pada plat rata bergerak di dalam ferrobendalir dengan syarat sempadan sedutan dan kesan gelincir. Perhatian tertumpu pada masalah olakan paksa dan campuran di dalam bendalir tak termampat. Tiga masalah yang dipertimbangkan ialah; (1) aliran olakan paksa MHD pada plat rata bergerak di dalam ferrobendalir dengan kesan sedutan dan gelincir peringkat kedua; (2) aliran olakan campuran MHD pada plat rata bergerak di dalam ferrobendalir dengan kesan sedutan dan gelincir; dan (3) aliran olakan campuran MHD pada plat rata bergerak di dalam ferrobendalir dengan kesan sinaran terma, sedutan dan gelincir peringkat kedua. Untuk menyelesaikan masalah ini, mulanya persamaan pembezaan separa berdimensi yang mengawal aliran lapisan sempadan dijelmakan menjadi persamaan tak berdimensi dengan menggunakan pemboleh ubah tak berdimensi yang sesuai. Persamaan ini kemudiannya dibentuk semula menghasilkan persamaan pembezaan biasa tak linear dengan menggunakan transformasi keserupaan. Sistem yang dihasilkan diselesaikan secara berangka menggunakan kaedah tembakan yang dilakukan dengan bantuan fungsi *shootlib* dalam perisian Maple. Kaedah ini dikaitkan dengan kaedah peringkat keempat Runge-Kutta

bersama dengan Newton-Raphson sebagai skim pembetulan. Seterusnya, jika terdapat penyelesaian yang tidak unik, analisis kestabilan dilakukan untuk mengenal pasti penyelesaian yang stabil, dengan melaksanakan penyelesai `bvp4c` di Matlab. Kesan parameter olakan campuran, parameter magnet, parameter sinaran, parameter bergerak, parameter pemindahan jisim, parameter permukaan gelincir peringkat pertama, parameter permukaan gelincir peringkat kedua dan pecahan isipadu ferrozarah pepejal ke atas halaju dan suhu tak berdimensi, serta pekali geseran kulit dan nombor Nusselt setempat dibincangkan dalam bentuk jadual dan grafik. Untuk kajian ini, keputusannya dipertimbangkan berdasarkan tiga ferrozarah utama, iaitu magnetit, kobalt ferit dan mangan-zink ferit di dalam cecair berasaskan air dan kerosin. Didapati bahawa parameter olakan campuran, parameter magnet, parameter bergerak, serta pecahan isipadu ferrozarah pepejal membantu meningkatkan pekali geseran kulit dan kadar pemindahan haba. Di samping itu, kehadiran sedutan dan sinaran meningkatkan kadar pemindahan haba, manakala faktor gelincir menyebabkan pengurangan besar kepada nilai pekali geseran kulit. Keputusan menunjukkan wujudnya penyelesaian dual dan ketiga untuk sesetengah julat bagi pelbagai parameter olakan campuran, bergerak (plat bergerak ke arah asal) dan pemindahan jisim (sedutan). Seterusnya, analisis kestabilan menunjukkan terdapat gangguan pereputan awal bagi penyelesaian pertama, sementara penyelesaian kedua dan ketiga menunjukkan gangguan pertumbuhan awal, yang mana menunjukkan bahawa penyelesaian pertama stabil dan secara fizikal dapat direalisasikan, sementara penyelesaian kedua dan ketiga tidak.

**STABILITY ANALYSIS OF MAGNETOHYDRODYNAMIC FLOW AND
HEAT TRANSFER OVER A MOVING FLAT PLATE IN FERROFLUIDS
WITH SLIP EFFECTS**

ABSTRACT

A study of the stability analysis on the boundary layer flow has become a great interest in the field of fluid dynamics. This analysis is essential because it helps to identify which solution is stable if there exists non-unique solutions in the computation. In this thesis, the stability analysis is applied on the problems of the steady, two-dimensional, laminar, magnetohydrodynamic (MHD) flow and heat transfer over a moving flat plate in ferrofluids with suction and slip boundary conditions. It aims attention on the problem of forced and mixed convection immersed in an incompressible fluid. The three problems considered are; (1) MHD forced convection flow over a moving flat plate in ferrofluids with suction and second-order slip effects; (2) MHD mixed convection flow over a moving flat plate in ferrofluids with suction and slip effects; and (3) MHD mixed convection flow over a moving flat plate in ferrofluids with thermal radiation, suction and second-order slip effects. In order to solve these problems, the dimensional partial differential equations that governed the boundary layer flows are first transformed into non-dimensional equations by using appropriate dimensionless variables. These equations are then reconstructed into the form of nonlinear ordinary differential equations by applying the similarity transformation. The resulting system is solved numerically using the shooting method which is done with the aid of *shootlib* function in Maple software. This method is associated with the Runge-Kutta fourth order method together with Newton-Raphson as a correction scheme. Further, if there are non-unique solutions, the stability analysis is performed to identify which solution

is stable, by implementing bvp4c solver in Matlab. The effects of the mixed convection parameter, magnetic parameter, radiation parameter, moving parameter, mass transfer parameter, first-order surface slip parameter, second-order surface slip parameter and volume fraction of solid ferroparticles on the dimensionless velocity and temperature, as well as the skin friction coefficient and local Nusselt number are discussed in the form of tabular and graphical presentation. For this present study, the results are considered based on three preferred ferroparticles, namely magnetite, cobalt ferrite and manganese-zinc ferrite in water- and kerosene-based fluids. It is found that the mixed convection parameter, magnetic parameter, moving parameter, as well as the volume fraction of solid ferroparticles help to enhance both skin friction coefficient and heat transfer rate. In addition, the presence of suction and radiation parameter serves the heat transfer rate to increase, while the slip factor provides an enormous reduction of the skin friction coefficient. The results display the existence of dual and triple solutions for certain range of the mixed convection, moving (a plate moving towards the origin) dan mass transfer (suction) parameters. Further, the stability analysis showed that there is an initial decay of disturbance for the first solution, while the second and third solutions showed an initial growth of disturbance, indicated that the first solution is stable and thus physically realizable, while the second and third solutions are not.

CHAPTER 1

INTRODUCTION

1.1 Introductory Remarks

Heat transfer is a study of energy transfer processes between material bodies solely as a result of temperature differences. These processes play a vital role and can be discovered in a great variety of practical situations. The problems of heat transfer confront the engineers and researchers in nearly every branch of science and engineering. The mechanism by which heat is transferred in a heat exchange or an energy conversion system is quite complex. There appear to be three rather basic and distinct modes of heat transfer namely, conduction, convection and radiation. The transfer of energy from the more energetic particles of a substance to the adjacent less energetic ones as a result of interactions between particles is called conduction. Further, convection is the mode of energy transfer between a solid surface and the adjacent liquid or gas that is in motion, and it involves the combined effects of conduction and fluid motion (Çengel, 2007). Thermal radiation, or simply radiation, is heat transfer in the form of electromagnetic waves as a result of the changes in the electronic configurations of the atoms or molecules (Kakaç and Yener, 1994).

There exists two ways of motion of heat transfer from a surface, either it is moving or stationary fluid. The boundary layer flow due to a moving flat plate is a relevant type of flow appearing in many industrial processes, such as manufacture and extraction of polymer and rubber sheets, paper production, wire drawing and glass-fiber production, melt spinning, continuous casting, and many more (Tadmor and Klein, 1970). Then,

the study of the flow and heat transfer over a moving flat plate in an electrically conducting fluid permeated by a uniform transverse magnetic field is of special interest. The subject of magnetohydrodynamic (MHD) has developed in many directions and industry has exploited the use of magnetic fields in controlling a range of fluid and thermal processes. Many studies of the influence of magnetism on electrically-conducting flows has been reported very often especially in the relation of MHD generator, pumps, meters, bearings and boundary layer control (Ishak et al., 2008). MHD appears that an understanding of the effect of an applied magnetic field on the flow and heat transfer is useful for the cooling process (Watanabe et al., 1995).

Recently, the magnetic convection of ferrofluids is of considerable interest in the applications of science and engineering. Magnetic nanofluids (ferrofluids) are a magnetic colloidal suspension consisting of base fluid and magnetic nanoparticles with a size range of 5 to 15 nm in diameter coated with a surfactant layer. The most often used magnetic material is single domain particles of magnetite, iron, or cobalt; and the base fluids such as water or kerosene. Ferrofluids are a unique material that has both the liquid and magnetic properties. In the absence of magnetic field, these fluids behave as normal nanofluids (Hayat et al., 2016). The advantage of the ferrofluids are that the fluid flow and heat transfer may be controlled by an external magnetic field which makes it applicable in various fields such as electronic packing, mechanical engineering, thermal engineering, aerospace and bioengineering (Mohammadpourfard, 2012).

In this present study, we focus on the stability analysis of MHD flow and heat transfer over a moving flat plate in ferrofluids with uniform heat flux, under the influence

of suction, first-order velocity slip, second-order velocity slip and thermal radiation. The flow is assumed to be laminar, steady, incompressible and two-dimensional. The analysis include: (1) formulation of the mathematical models to obtain the governing boundary layer flow and heat transfer equations for the new models; (2) similarity transformation; (3) numerical computation using shooting method in Maple software; (4) analysis of stability using function of bvp4c in Matlab. Effects of various pertinent parameters on the skin friction coefficient, local Nusselt number, velocity and temperature profiles are thoroughly analysed and examined according to each problems that are discussed.

1.2 Magnetohydrodynamic (MHD)

Magnetohydrodynamic (MHD) is a branch of study about fluid dynamics where magnetic fields are important in the flow and the fluid must be electrically conducting. The term of “magnetohydrodynamic” comes from the word magneto (magnetic field), hydro (water) and dynamics (movement). It was initiated by the Swedish Physicist named Hannes Alfvén who received the Nobel Prize in Physics in 1970. The subject is also sometimes called ‘hydromagnetic’ or ‘magneto-fluid dynamic’ (Roberts, 1987).

These fluids consist of liquid metals (such as gallium, mercury, molten iron), salt water and ionized gases or plasmas (such as the solar atmosphere). MHD comprises on the phenomena where the velocity field \mathbf{V} and the magnetic field \mathbf{B} become couples in an electrically conducting fluid. The magnetic field induces an electric current of density \mathbf{J} in the moving conductive fluid (electromagnetism). The current that is induced forms forces on the liquid and modifies the magnetic field. Each unit volume of

the fluid gaining the magnetic field involves the force of MHD named $\mathbf{J} \times \mathbf{B}$ or known as Lorentz force. Then, the set of equations describing MHD flows are a combination between Navier-Stokes equation of fluid dynamics and Maxwell's equation of electro-magnetism.

1.3 Heat Transfer

Heat can be described as energy transferred due to a temperature difference between two systems. It always occur from the higher temperature region to the lower temperature region. Heat transfer is usually encountered in many aspects of our daily life besides in engineering systems such as human body, car radiators, air-conditioning systems, power plants, refrigeration systems and many more. There are three basic modes of heat transfer, namely, conduction, convection, and radiation. An extensive study has been conducted in the convection mode in heat transfer since it takes place with the motion of the fluid. Let's consider each of these three modes individually.

1.3.1 Conduction

Conduction is the transfer of heat from one part of a body at a higher temperature to another part of the same body at a lower temperature, or from one body at a higher temperature to another body in physical contact with it at a lower temperature (Rohsenow et al., 1998). The process of conduction generally happened at the level of molecular and engages the energy transfer from the more active molecules to the one with a lower level of energy. Conduction can take place in solids, liquids and gases. In gases, the average kinetic energy of molecules in the higher-temperature regions is greater compared to those in the lower-temperature regions. The more active

molecules, being in constant and random motion, periodically collide with molecules of a lower energy level and exchange energy and momentum. Moreover, in liquids, the molecules are more closely spaced than in gases, although the process of molecular energy exchange is approximately identical to that in gases. In solids, the conduction is due to the combination of vibrations of the molecules in a lattice and the energy transport by free electron.

The heat flux \mathbf{q} represents a current of heat which is also known as thermal energy that flows in the direction of the steepest temperature gradient and is defined in more general statement of Fourier's Law as (Rohsenov et al., 1998)

$$\mathbf{q} = -k\nabla T, \quad (1.1)$$

where k denotes the thermal conductivity, ∇ is a Laplacian operator ($\nabla = \mathbf{i}\frac{\partial}{\partial x} + \mathbf{j}\frac{\partial}{\partial y}$, for two-dimensional where x and y are the Cartesian coordinate measured along and normal to the plate, respectively) and T is the scalar temperature field. The minus sign represents the fact that heat is transferred in the direction of declining temperature.

The examples of conduction process in our daily life including a spoon in a cup of hot soup becomes warmer because the heat from the soup is conducted along the spoon, the earth warms from the light of the sun as the heat is conducted through the atmosphere, an ice cube will melt if one holds in the hand since the heat is being conducted from the hand into the ice cube. Metals become good conductors of heat compared to the non-metals because they contain free electrons which help to transfer the heat from the hot to the cold end faster. The metals that can be used including

aluminum, bronze, copper, gold, iron, mercury and others.

1.3.2 Convection

Convection or sometimes identified as convective heat transfer is the mode of energy exchange that is customarily related with heat crossing a boundary or surface between a solid and a fluid due to the temperature difference. The fluid can be considered as fluids and gases at a low or high temperature (Rolle, 2014). The fluids and gases can transfer heat very quickly by convection even though they are not good conductors of heat. Convection appeared widely in our environment and in most engineering services including cooking, the cooling of the electronic components in a computer, the heating and cooling of buildings, the cooling of the cutting tool during a machining operation and many more. Convective heat transfer is usually classified into three basic processes namely, free convection, forced convection and mixed convection.

1.3.2(a) Free Convection

Free convection is also referred as natural convection which takes place if the fluid motion is caused by buoyancy forces that are induced by density differences due to the variation of temperature in the fluid. For example, heat transfer occurs when a cup of hot water is exposed by the air surrounding without any external force.

1.3.2(b) Forced Convection

On the other hand, the forced convection is present whenever the fluid motion is forced to flow over the surface by external means such as a pump, a blower, a fan or some similar devices. The examples of forced convection are air conditioning, heat

exchangers, central heating and others. The forced convection is more capable than the natural convection because of the faster velocity of the currents and the buoyancy has little impact on the direction of flow.

1.3.2(c) Mixed Convection

Mixed convection is a combination of free and forced convection due to the effect of the buoyancy force in forced convection or the effect of forced flow in free convection becomes significant. Mathematically, the mixed convection flow is identified by the buoyancy or mixed convection parameter, $\omega = Gr/Re^n$, where Gr is the Grashof number, Re is the Reynolds number and $n(> 0)$ is a constant subject to the conditions of surface heating and fluid flow configuration. Meanwhile, the parameter ω presents a measure of flow significance between free and forced convection. The system of mixed convection is expressed as the range $\omega_{min} \leq \omega \leq \omega_{max}$ where ω_{min} and ω_{max} are the lower and the upper bounds of mixed convection flow regime, respectively.

1.3.3 Radiation

Radiation or also known as thermal radiation is an electromagnetic radiation diffused by a body by virtue of its temperature and at the expense of its internal energy (Rohsenow et al., 1998). In other words, the thermal radiation emitted as a result of energy transitions of molecules, electrons, and atoms of a substance. Radiation is dissimilar from conduction and convection since it does not need the existence of a material medium to take place. All substances from solids as well as fluids and gases are capable of occurring in radiation transfer.

Radiation provides extensively to energy transfer in combustion chambers, furnaces, fires and to the emission of energy from a nuclear explosion. In order to achieve great thermal efficiency, some devices are created to perform at high-temperature levels. Therefore, radiation must be considered in examining the effects of thermal in engines, rocket nozzles, power plants and high-temperature heat exchangers (Siegel and Howell, 2002).

1.4 Nanofluids

Nanofluids are a dilute liquid suspensions of nanoparticles with the size range under 100 nm in heat transfer fluid (Minkowycz et al., 2013). Figure 1.1 illustrates a schematic cross-section of the proposed nanofluids consisting of nanoparticles, base fluid, and nanolayers at the interface of solid or fluid (Sridhara et al., 2009).

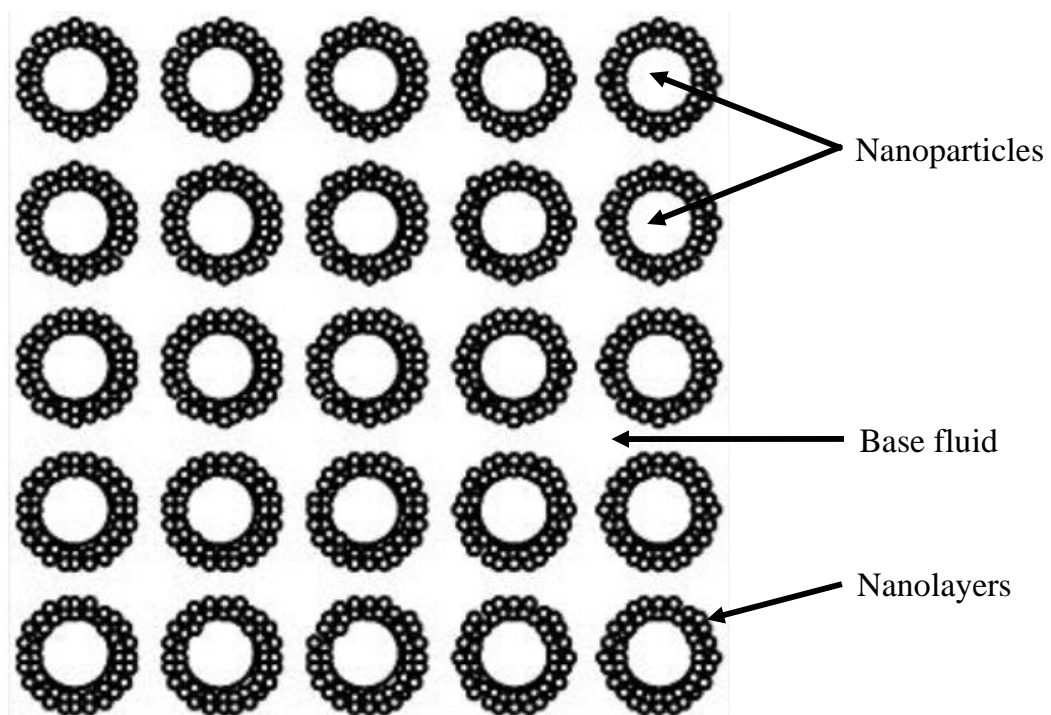


Figure 1.1: Schematic cross-section of nanofluids structure (Sridhara et al., 2009)

Nanoparticles are created from various materials such as oxide ceramics (aluminium oxide Al_2O_3 , copper oxide CuO), nitride ceramics (aluminium nitride AlN , silicon nitride SiN), carbide ceramics (silicon carbide SiC , titanium carbide TiC), metals (copper Cu , silver Ag , gold Au), semiconductors, carbon nanotubes and composite materials such as alloyed nanoparticles or nanoparticle core-polymer shell composites (Uddin et al., 2012). The base fluids which mostly applied in the preparation of nanofluids are the common heat transfer fluids such as water, oil and ethylene glycol (Chamkha et al., 2013). In solid liquid mixture, the liquid molecules close to a solid surface are known to form a layered structure and this layer acts as nanolayer. The solid-like nanolayer acts as a thermal bridge between a solid nanoparticle and a bulk liquid and so is the key of enhancing the thermal conductivity (Sridhara et al., 2009).

Based on the literature, nanofluids have been initiated to acquire enhanced thermophysical properties such as thermal conductivity, thermal diffusivity, viscosity and convective heat transfer coefficient compared to the base fluids (Kakaç and Pramuanjaroenkij, 2009; Wong and Leon, 2010). Choi (1995) was the first person who used the term nanofluids. He studied the problem of nanofluids which help to exhibit the thermal properties of fluids with nanoparticles. Nanofluids can be considered to be the next generation heat transfer fluids because they offer exciting new possibilities to enhance heat transfer performance compared to pure liquids (Wang and Mujumdar, 2008).

There are a few nanofluid models available in the literature. Among the well-known models are the models which are proposed by Khanafer et al. (2003), Buongiorno (2006), Tiwari and Das (2007) and Nield and Kuznetsov (2009). In this study,

the model of Tiwari and Das is employed in order to observe the behavior of nanofluids due to the presence of nanoparticle volume fraction. This model is developed by using Brinkman (1952) model for viscosity and Maxwell-Garnetts model for thermal conductivity. These models are limited to spherical nanoparticles and do not applicable for other shapes of nanoparticles. Many researchers then implemented this model in their studies such as Ahmad and Pop (2010), Ahmad et al. (2011), Sheremet et al. (2014), Ul Haq et al. (2014), Sheikholeslami and Ganji (2014), Nadeem et al. (2014), Sheremet et al. (2015), Ghalambaz et al. (2015), Sheremet et al. (2016), Dinarvand et al. (2017), Mabood et al. (2017) and Aghamajidi et al. (2018).

1.5 Ferrofluids

The research about flow analysis of nanofluids with the interaction of magnetic field has increased enormously. Magnetic nanofluids which are also known as ferrofluids are colloidal suspensions of magnetic nanoparticles with a size range of 5 - 15 nm in diameter scattered in non-conducting base fluid (Sheikholeslami and Rashidi, 2015). The magnetic nanoparticles which are commonly used include magnetite, cobalt, and ferrite while the base fluids such as water, kerosene, heptane, and hydrocarbons (Rashad, 2017a). Ferrofluids were originally invented by Papell (1965) at the NASA (National Aeronautics and Space Administration) Research Center and his first work about the synthesis of ferrofluids discovered the method for controlling fluids in space. In addition, ferrofluids are important in order to absorb electromagnetic field to enhance the heat transfer.

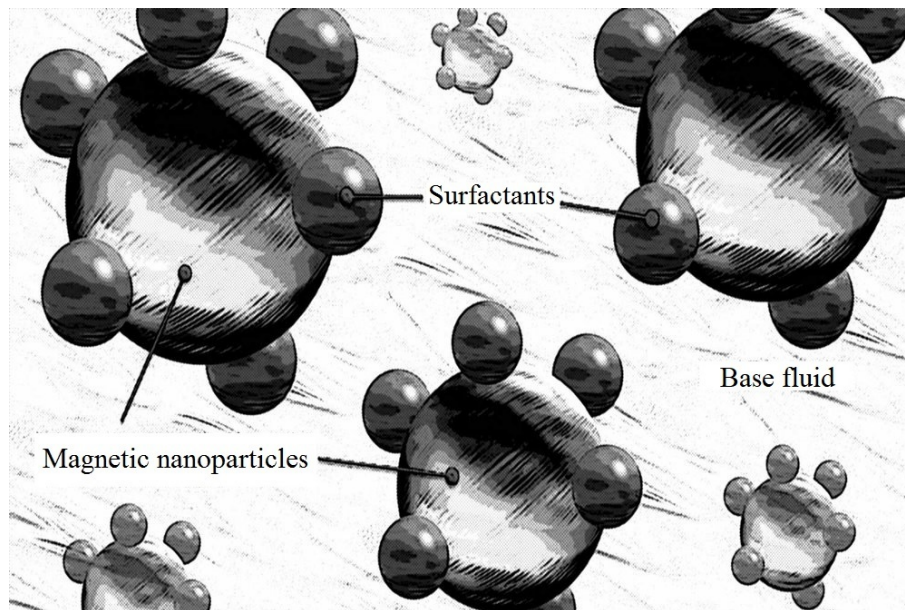


Figure 1.2: Components of ferrofluids (Rene, 2014)

Figure 1.2 shows the composition of ferrofluids which have three basic components including the magnetic nanoparticles, surfactants, and base fluid. The surfactants can be illustrated as soap-like materials that work to coat the magnetic nanoparticles and keep them from being engaged to each other. Moreover, the base fluid will encourage in determining the thickness and viscosity of the ferrofluids, subjected to the point that the magnetic properties are solely due to the suspended particles (Kaiser and Rosensweig, 1969). Ferrofluids are generally employed to deal with the fluid flow and heat transfer rate. They find applications in the field of aerospace, aeronautical, industrial engineering, medical, science and technology (Rosensweig, 1985; Hiegeister et al., 1999).

1.6 Boundary Layer Theory

The concept of boundary layer was first postulated by a German physicist, Ludwig Prandtl in 1904. His companion paper entitled "On the motion of fluids of very small viscosity" had been presented at the Third International Congress of Mathematicians

took place at Heidelberg. It was proved to be one of the most influential fluid-dynamics papers ever written (Acheson, 1990; Anderson, 2005). Ludwig Prandtl demonstrated that the field of flow past a body can be divided into two principal areas as follows (Schlichting, 1968; Nag, 2011):

- (a) A very thin layer in the neighborhood of the body which is called boundary layer where friction plays an essential part and cannot be ignored.
- (b) The remaining region outside this layer where the friction may be neglected and the flow was essentially the inviscid flow. The fluid is considered to be ‘ideal’, that is nonviscous and incompressible.

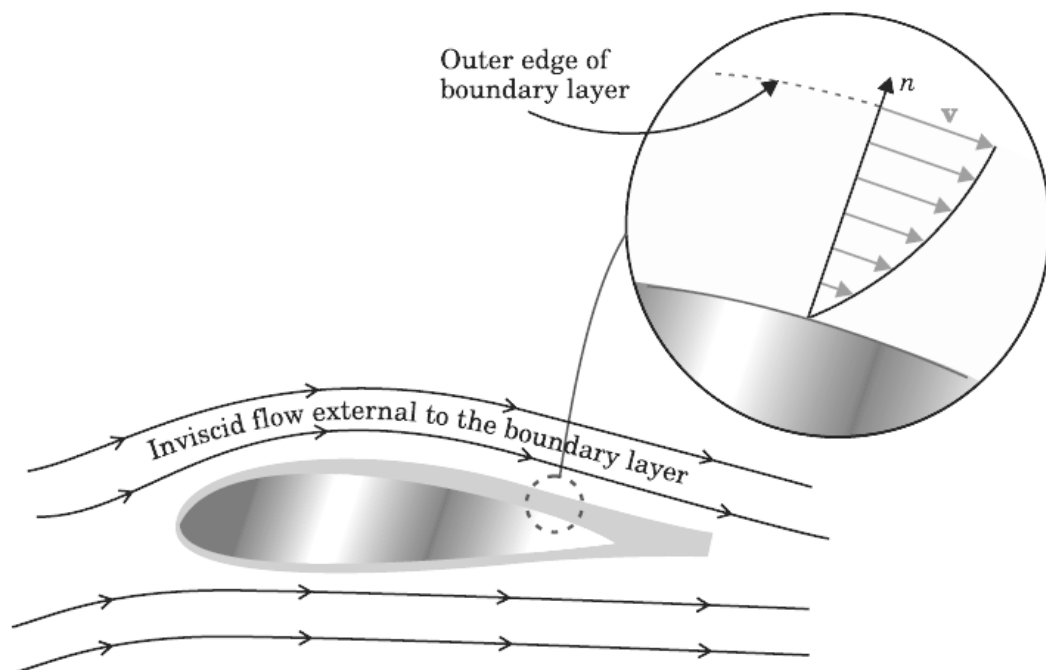


Figure 1.3: Regions of the fluid flow (Anderson, 2005)

This concept of the boundary layer is illustrated in Figure 1.3. The enlargement of the boundary layer presents how the flow velocity v changes, as a function of normal distance n , from zero at the surface to the full inviscid-flow value at the outer edge

(Anderson, 2005). When a fluid flows over a body, the velocity and temperature distribution at the instantaneous vicinity of the surface firmly gives the influence to the heat transfer by convection. The boundary layer can be divided into two different kinds concerning the velocity boundary layer and the thermal boundary layer, as displayed in Figure 1.4. A brief description of each type is discussed as follows:

(a) Velocity boundary layer

The region in the fluid is developed due to an interaction between the fluid and the surface, where the x -component velocity u grows up from zero at the surface (no slip condition) to an asymptotic value U_∞ . This region of large velocity gradient is known as the velocity boundary layer where δ_V is the velocity boundary layer thickness. This layer is identified by the velocity gradient and the shear stress.

(b) Thermal boundary layer

The region in the fluid is formed due to the presence of temperature difference between the fluid and the surface where the temperature varies from the temperature at wall T_w to the value of external flow T_∞ . This region with large temperature gradient is known as the thermal boundary layer where δ_T denotes the thermal boundary layer thickness. This layer is identified by the temperature gradient and the heat transfer.

There are several excellent books which described briefly the theory of boundary layer in the literature including Moore (1956), Schlichting (1968), Tritton (1988), Faber (1995), Oleinik and Samokhin (1999), Sobey (2000), and others.

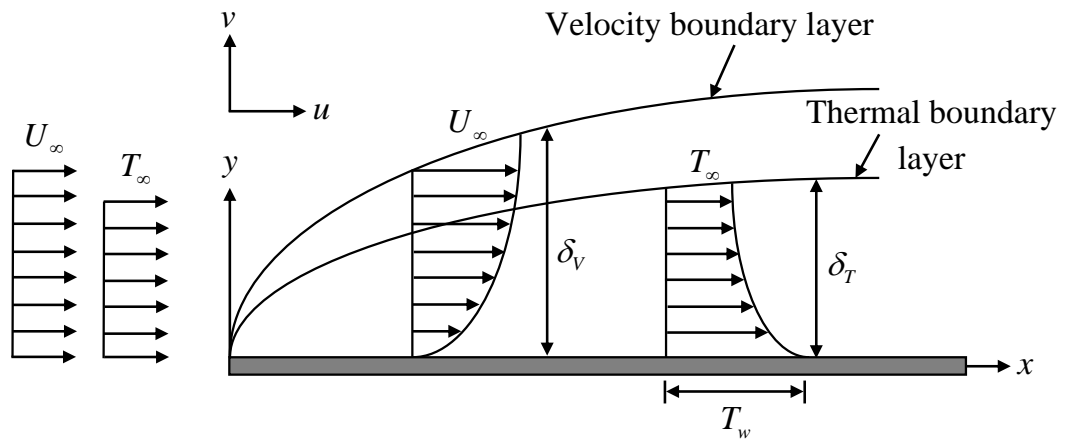


Figure 1.4: Velocity and thermal boundary layers (Malvandi et al., 2013)

1.7 Suction

Suction has been well recognised as a common method of controlling the boundary layer flow. Suction of fluid through the bounding surfaces, as, for example, in mass transfer cooling, it can significantly change the flow field and, as a consequence, affect the rate of heat transfer from the bounding surfaces. In general, suction tends to increase the skin friction and heat transfer coefficient (Jha and Aina, 2016). Instead, it plays an important role to enhance cooling of the system and can help to delay the transition from laminar flow. It is often necessary to postpone separation of the boundary layer to reduce drag and attain high lift values (Pop and Watanabe, 1992).

Practically, the behavior of a laminar boundary layer can be influenced by suction of fluid at the solid surface. Suction removes decelerated fluid particles from the boundary layer before they have a chance to cause flow separation (Burmeister, 1993). In other words, suction contributes to the stability of the boundary layer by delaying the transition so that the flow is laminar rather turbulent. A major benefit of suction on airfoils is to reduce drag. Also, suction can be applied by using permeable surface, porous surface and surfaces with multiple series of finite slots. The implementation

of suction requires the surface to have holes which can be clarified to refer as perforations, slots and porous sections. In addition, the holes are essential to help sucking the portion of the boundary layer that is closest to the wall.

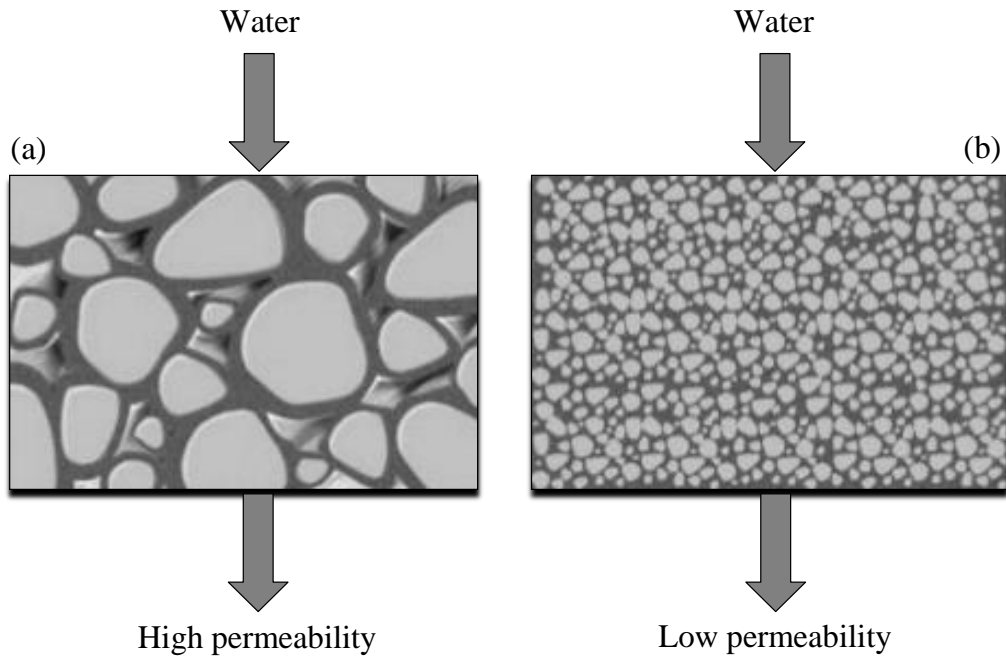


Figure 1.5: Permeability, (a) rock and (b) sand (Edwards, 2016)

Permeability is a measure of the ability of a substance to allow another substance to pass through it, especially the ability of a porous rock, sediment, or soil to transmit fluid through pore spaces and cracks. It is also known as the property or condition of being permeable. From Figure 1.5, we can see that the rock has a high permeability because of large pore size and this gives rock the ability to drain a lot of water. Hence, the medium are permeable by the cause of the presence of interrelated gaps through which water can move from high energy points to low energy points.

1.8 Slip Condition

The study between the fluid and the solid boundary conditions in recent years has seen a renewed interest. The slip length, which is a simple measurement of the slip, is apparently the most commonly used parameter to characterize the slip. In 1823, Navier proposed a more general boundary condition, which takes into account that the fluid may slip on the surface of the solid. Navier's proposed condition assumes that the velocity, $u(x, y)$, at a solid surface is proportional to the shear stress, $\frac{\partial u}{\partial y}$, at the surface (Mehmood and Ali, 2007; Ananthaswamy et al., 2017) such that

$$u(x, y) = L_s \frac{\partial u}{\partial y} \quad (1.2)$$

where L_s is the slip length or slip coefficient. If $L_s = 0$, then the general assumed no-slip boundary condition is obtained. If L_s is finite, fluid slip occurs at the wall but its effect depends upon the length scale of the flow. The above relation states that the velocity of the fluid at the plates is linearly proportional to the shear stress at the plate. Figure 1.6 illustrates the slip length, L_s , for simple shear flow along a flat plate. In physical terms, the slip length can also be interpreted as the fictitious distance inside the solid where fluid velocity extrapolates linearly to zero (Lauga, 2004).

The degree of slip at the boundary depends on a number of interfacial parameters including the strength of the liquid-solid coupling, the thermal roughness of the interface, and the commensurability of wall and liquid densities (Thompson and Robbins, 1990). These findings have led to a new understanding of stick-slip phenomena in boundary lubrication and have revealed the sensitivity of liquid spreading to microstructure at the liquid or solid interface (Thompson and Troian, 1997).

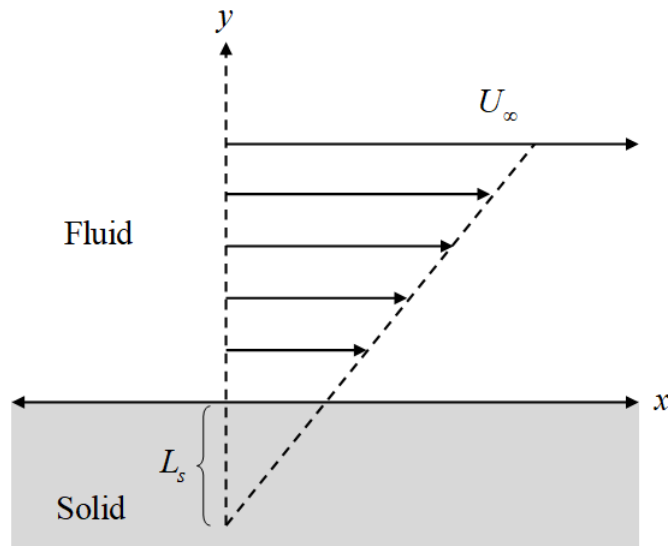


Figure 1.6: Slip length, L_s , for simple shear flow along a flat plate (Thompson and Troian, 1997; McCormack, 2012)

In 1879, Maxwell used the kinetic theory of gases to identify the slip condition. The fluid velocity at the solid surface is assumed to be proportional to the shear rate at the surface, and the proportionality constant has dimensions of length (McCormack, 2012). The Navier and Maxwell slip boundary conditions are then widely used in the study of diverse engineering applications.

1.9 Dimensionless Parameters

Phenomena in the fluid mechanics depend on the dimensionless parameters, which are a set of dimensionless quantities that have an important role in the behaviour of fluids. There are many reasons for using the dimensionless parameters including they allow to solve the problem easily, tell how the system will behave and allow for comparisons between very different system. Among the parameters involved are the Prandtl number Pr , Reynolds number Re , Grashof number Gr , Nusselt number Nu , Eckert number Ec and Knudsen number Kn . The definitions and details of these dimensionless parameters are discussed in Sections 1.9.1–1.9.6.

1.9.1 Prandtl Number

Prandtl number is a dimensionless parameter which is named after the German physicist, Ludwig Prandtl. It is defined as the ratio of molecular diffusivity of momentum to the molecular diffusivity of heat as follows (Çengel, 2007):

$$\text{Pr} = \frac{\text{molecular diffusivity of momentum}}{\text{molecular diffusivity of heat}} = \frac{\nu}{\alpha} = \frac{\mu/\rho}{k/\rho C_p} = \frac{\mu C_p}{k}$$

where ν is the kinematic viscosity, α is the thermal diffusivity, μ is the coefficient of kinematic viscosity, ρ is the density of the fluid, C_p is the specific heat at constant pressure and k is the thermal conductivity. Table 1.1 presents the values of Prandtl number that is commonly used in heat transfer either in the calculation of free or forced convection. The Prandtl numbers of fluids range from less than or equal to 0.03 for

Table 1.1: Prandtl number of various fluids

Fluid	Pr
Liquid metals	0.004 - 0.030
Gases	0.7 - 1.0
Water	1.7 - 13.7
Light organic fluids	5 - 50
Oils	50 - 100000
Glycerine	2000 - 100000
Heavy oils	> 100000

liquid metals to more than 100000 for heavy oils. Moreover, the Prandtl numbers of gases are about 1, which indicates that both momentum and heat dissipate through the fluid at about the same rate. Heat diffuses very quickly in liquid metals ($\text{Pr} \ll 1$) and very slowly in oils ($\text{Pr} \gg 1$) relative to momentum.

1.9.2 Reynolds Number

The transition from laminar to turbulent flow depends on the surface geometry, surface roughness, flow velocity, surface temperature, and type of fluid, among other things. After exhaustive experiments in the 1880s, Osborn Reynolds discovered that the flow regime depends mainly on the ratio of the inertia forces to viscous forces in the fluid. This ratio is called the Reynolds number and can be expressed as (Çengel and Cimbala, 2006; Çengel, 2007)

$$\text{Re} = \frac{\text{inertia forces}}{\text{viscous forces}} = \frac{\rho UL}{\mu} = \frac{UL}{\nu}$$

where U is the velocity of the fluid with respect to the object, L is the characteristic length of the geometry and $\nu = \frac{\mu}{\rho}$ is the kinematic viscosity of the fluid. Laminar flow generally occurs when dealing with small Reynolds number, where viscous forces are dominant and is indicated by consistent and smooth motion with no distraction in the layers. However, the turbulent flow occurs for large Reynolds number, where inertial forces are dominant and is influenced by chaotic property changes.

1.9.3 Grashof Number

The Grashof number is the dimensionless parameter used in the correlation of heat and mass transfer which demonstrates the ratio of the buoyancy forces to the viscous forces. It frequently arises in the study of situations involving natural (free) or mixed convections. It is named after a German engineer, Franz Grashof and is defined as

(Bianco et al., 2015)

$$\text{Gr} = \frac{\text{bouyancy forces}}{\text{viscous forces}} = \frac{g\beta(T_w - T_\infty)L^3}{\nu^2}$$

where g is the gravitational acceleration, β is the coefficient of volume expansion, T_w is the temperature of the surface and T_∞ is the temperature of the fluid sufficiently far from the surface. Grashof number contributes a special principle in evaluating whether the flow of fluid is laminar or turbulent in natural or mixed convections. Furthermore, it indicates that the problem involved both free and forced convection when the surface is subjected to the external flow. It may be useful to apply the ratio of the Grashof number to the square of Reynolds number such that the effects of free convection are usually insignificant when $\frac{\text{Gr}}{\text{Re}^2} \ll 1$ and conversely the effects of forced convection may be negligible for $\frac{\text{Gr}}{\text{Re}^2} \gg 1$. Otherwise, when $\frac{\text{Gr}}{\text{Re}^2} \approx 1$, both effects that are combined free and forced convection are important and have to be taken into account.

1.9.4 Nusselt Number

The Nusselt number is the dimensionless parameter which describes convective heat transfer coefficient and it is named after a German engineer, Wilhelm Nusselt. It is illustrated as (Çengel, 2007)

$$\text{Nu} = \frac{\text{convection heat transfer}}{\text{conduction heat transfer}} = \frac{h\Delta T}{k\Delta T/L} = \frac{hL}{k}$$

where h is the heat transfer coefficient and ΔT is the driving force for the heat transfer. The convection becomes more effective if the Nusselt number is large. Meanwhile, if $\text{Nu} = 1$, it indicates that the heat transfer across the layer by pure conduction.

1.9.5 Eckert Number

The Eckert number is named after a scientist, Ernst Rudolph Georg Eckert in the early 1950's. It is beneficial in determining the relative importance in the heat transfer situation of the kinetic energy of a flow. The Eckert number is defined as the ratio of the kinetic energy to the enthalpy (or the dynamic temperature to the temperature) driving force for heat transfer (Çengel and Cimbala, 2006)

$$Ec = \frac{\text{kinetic energy}}{\text{enthalpy}} = \frac{U^2}{C_p \Delta T} = \frac{U^2}{C_p (T_w - T_\infty)}$$

where ΔT is the driving force for heat transfer or can be denoted as the wall temperature minus free stream temperature. The terms in the energy equation representing the effects of viscous dissipation, pressure changes and body forces on the energy balance are ignored when the Eckert number is small, i.e. $Ec \ll 1$. The energy equation then reduces to a balance between conduction and convection. When the Eckert number is large, i.e. $Ec \gg 1$, the heat transfer is zero which means that the wall is adiabatic. Further, the Eckert number for zero heat transfer is independent of the pressure gradient parameter (Rogers, 1992).

1.9.6 Knudsen Number

A dimensionless parameter known as Knudsen number is the ratio of the mean free path length of the molecules of a fluid to a characteristic length (Çengel and Cimbala, 2006; Bianco et al., 2015)

$$Kn = \frac{\text{mean free path length}}{\text{characteristic length}} = \frac{\lambda_m}{L}$$

where λ_m is the mean free path and L is the characteristic length. It describes the degree of departure from continuum. Usually when $\text{Kn} > 0.01$, the concept of continuum does not hold good. Beyond this critical range of Knudsen number, the flows are known as slip flow ($0.01 < \text{Kn} < 0.1$), transition flow ($0.1 < \text{Kn} < 10$) and free-molecule flow ($\text{Kn} > 10$).

The Knudsen number helps determine whether statistical mechanics or the continuum mechanics formulation of fluid dynamics should be used to model a situation. If the Knudsen number is near or greater than one, the mean free path of a molecule is comparable to a length scale of the problem, and the continuum assumption of fluid dynamics is no longer a good approximation. In such cases, statistical methods should be used.

1.10 Motivations of Study

This section discusses the three papers that motivate the research undertaken in this study. First, the work by Khan et al. (2015) who studied the problem of flow and heat transfer of ferrofluids along a plate subjected to uniform heat flux and slip velocity in which a magnetic field was applied in the transverse direction to the plate. This work considered three different kinds of magnetic nanoparticles (magnetite Fe_3O_4 , cobalt ferrite CoFe_2O_4 , Mn-Zn ferrite $\text{Mn-ZnFe}_2\text{O}_4$) within two base fluids (kerosene and water). They concluded that the magnetic field tends to increase both skin friction and heat transfer rate, while the effect of the slip parameter is to reduce friction and increase the heat transfer. Furthermore, kerosene-based Fe_3O_4 provides the higher heat transfer rate at the wall as compared to the kerosene-based CoFe_2O_4 and $\text{Mn-ZnFe}_2\text{O}_4$. The

second paper that contributes to the research on this thesis is the stability analysis for the problem of mixed convection stagnation point flow past a vertical flat plate with a second order slip, when the plate is maintained at a variable heat flux. This work has been revealed by Roşca and Pop (2013a) and the solutions predicts that dual solutions exist for the opposing flow case with curves which bifurcate at the critical point. The second-order slip affects considerably the flow and heat transfer characteristics and the stability analysis showed that the upper branch solution is stable and physically realizable while the lower branch solution is unstable.

The last one is the work by Ishak (2009) who developed the effects of thermal radiation on the steady laminar boundary layer flow over a moving plate in a moving fluid. It should be remarked that the dual solutions exist when the plate and the fluid move in the opposite direction. Meanwhile, the existence of thermal radiation will help to reduce the heat transfer at the surface. Therefore, motivated by these works, we would like to extend the work in finding the stability analysis of MHD flow and heat transfer over a moving flat plate in ferrofluids with thermal radiation, suction and slip effects, by using three selected ferroparticles (Fe_3O_4 , CoFe_2O_4 , $\text{Mn-ZnFe}_2\text{O}_4$) in water- and kerosene-based ferrofluids.

1.11 Problem Statement

A stability analysis is motivated by interest in numerical procedures for determining which solution is linearly stable and physically realizable if the system of equations possesses non-unique (dual or triple) solutions. Many publications have shown that dual and triple solutions are associated by the buoyancy forces in the free or mixed

convection, and moving surfaces. It is worth mentioning that Ridha (1996) has shown for a number of two-dimensional mixed convection examples that dual solutions are associated not only with opposing flow situations, but they exist also for assisting flow regime (Pop and Ingham, 2001). With regards to the moving surfaces, Bachok et al. (2010) found dual solutions of the boundary layer equations for the flow of nanofluids over a moving surface in a flowing fluid.

Some previous studies including Turkyilmazoglu (2012), Rohni et al. (2013), Bachok et al. (2013) and Singh and Chamkha (2013) have mentioned the existence of dual (first and second) and triple (first, second and third) solutions. These studies conclude that the first solution is physically stable and occur in practice, whilst the second and third solutions are physically unstable. Although the second and third solutions are unstable and deprive of physical significant, it is still of mathematical interest since the solutions are also the solutions to the system of differential equations. The second and third solutions may have more realistic meaning in other situations (Ishak, 2014a).

In order to verify this postulate, the stability analysis has to be performed to identify which solution is stable and physically realizable if there are dual or triple solutions. This analysis showed that there is an initial decay for the first solution, while there is an initial growth of disturbances for the second and third solutions. According to the literature, such kind of dual solutions have been first studied by Merkin (1985) for the mixed convection flow past a vertical plate embedded in a porous medium. Then, this analysis has been applied by Weidman et al. (2006), Merrill et al. (2006), Harris et al. (2009), Postelnicu and Pop (2011), Nazar et al. (2014), Roşca et al. (2014a), Ismail et al. (2016), as well as Yasin et al. (2017). These studies were reported for